Invited Paper

Application of dilute boron B(Al,In,Ga)N alloys for UV light sources

S. Gautier[1], M.Abid[2], T.Moudakir[3], G. Orsal[1], A. En Naciri[4], K. Pantzas[2], F. Jomard[5], P. L. Voss[2], D. J. Rogers[6], F. Hosseini Teherani[6] and A. Ougazzaden[2].

(1) LMOPS – EA4423, Université Paul Verlaine de Metz and SUPELEC, UMI 2958 Georgia Tech-CNRS, France.
(2) Georgia Institute of Technology / GTL 2-3 rue Marconi, 57070 METZ, France - UMI 2958 Georgia Tech-CNRS
(3) Supélec / UMI 2958 Georgia Tech-CNRS, 2 rue E. Belin, 57070, Metz, France
(4) Laboratoire de Physique des milieux denses (LPMD), Université Paul Verlaine-Metz, 1 boulevard Arago, 57070 Metz, France
(5) Laboratoire de Physique des Solides et de Cristallogénèse (LPSC) UMR 8635 CNRS, Université de Versailles-Saint-Quentin1, place Aristide Briand, 92195 Meudon Cedex France.
[6] Nanovation, 103 bis rue de Versailles, 91400, Orsay, France.

ABSTRACT

In the last decades, development of the (Al,Ga,In)N materials has led to new generations of opto- and micro-electronic devices. More recently, novel B(Al,Ga,In)N alloys have been proposed for optical applications in the UV range. Since material containing boron possesses unique properties, the B(Al,Ga,In)N materials system is expected to permit the design of improved and/or novel devices. To evaluate this potential, an improved knowledge of the physical properties of these new materials will be required, however.

In this work, investigation of optical, structural, and compositional properties of low-boron content BGaN and BAlN ternary and BInGaN quaternary materials grown through Metalorganic Vapor Phase Epitaxy (MOVPE) are presented. It is shown that inclusion of a small amount of boron strongly affects the optical properties allowing the fabrication of BGaN-based Distributed Bragg Reflectors (DBRs) or Distributed Bragg Confinement layers (DBCs) with large refractive index contrast. Indeed, 1% of boron in BGaN/GaN multilayer structures gives a refractive index contrast of more than 0.1, which is equivalent to that of AlGaN/GaN containing 22% aluminum. The potential of boron-based material technology is illustrated for visible range solar cells applications through the example of BInGaN with good crystalline quality grown on ZnO buffered silicon substrates. It was found that through boron introduction, reduced lattice mismatch, and thus reduced tensile strain, could be obtained for high In contents.

Keywords: BGaN, BAlN, MOVPE, Ellipsometry, Distributed Bragg Mirrors

1. INTRODUCTION

Group III-nitrides such as GaN, AlN, and InN and their related alloys have been successfully commercialized as materials for microelectronic and optoelectronic devices. However, there is still room for innovation. Recently, a new class of alloys has been proposed, based on the introduction of boron into "classical" (AlInGa)N in order to extend the possibilities of strain and bandgap engineering in device structures.

Indeed, B(Al,Ga,In)N alloys offer the promise of novel applications, through the combination of the numerous unique properties of BN with the theoretical possibility of lattice matched growth with GaN, AlN, SiC or ZnO substrates.

Oxide-based Materials and Devices II, edited by Ferechteh Hosseini Teherani, David C. Look, David J. Rogers,
Proc. of SPIE Vol. 7940, 79400X · © 2011 SPIE · CCC code: 0277-786X/11/$18 · doi: 10.1117/12.884524

Examples of applications are: i) BAlGaN based active regions for UV-optoelectronic devices on AlN or SiC substrates[1], ii) BGaN/GaN and BAlN/AlN distributed reflectors (DBRs) or Distributed Bragg Confinement layers (DBCs) iii) BAlGaN nuclear detectors, which take advantage of the high sensitivity of the boron atoms to gamma radiation[2] and iv) BInGaN based third generation solar cells[3] in the visible range, potentially grown lattice-matched on GaN or ZnO template substrates.
The latter of these applications holds potential for low cost, third generation photovoltaic applications in two ways: i) the possibility to engineer the bandgap energy and the lattice parameter independently, for example, in the tailoring of a cell to lattice-match a ZnO template. ii) The possibility of using thin ZnO templates as sacrificial layers whereby nitride layers can be released from expensive or insulating substrates and wafer-bonded onto a substrate of choice[4] (since ZnO can be easily etched by most diluted acids or alkalis while nitrides cannot).
Although boron-containing alloys hold great potential, there are several hurdles to overcome in their fabrication. These include issues related to the phase separation[5] or spinodal decomposition[6], both of which can occur at high boron concentrations. It is generally accepted that true B(Al,Ga,In)N alloys without nanoclustering are not attainable above a few percent of boron. For instance, even with optimized growth conditions, BGaN alloys grown by MOVPE have not shown boron contents over 3.6%[7].
In addition, only a few studies, to date, report on “dilute boron” alloys (low boron content) and their physical properties are still relatively unexplored. There is, therefore, still a need for more research in order to better understand and improve the quality of these materials.
After giving the epitaxial growth conditions, this paper first of all reports on measurements of the optical properties of B(Al,Ga,In)N alloys, based on the analysis of single layers of dilute boron nitride alloys. Secondly, initial progress towards the growth of Distributed Bragg Reflectors using BGaN/GaN or BAlN/AlN structures will be presented. Third, HR-XRD and SIMS measurements on BInGaN quaternary materials grown on ZnO-buffered silicon for solar cells applications will be discussed.

2. GROWTH

All the nitride layers were grown using Metal Organic Chemical Vapor Phase Epitaxy (MOVPE). As the growth conditions for BGaN and BAlN alloys differ from those for BInGaN, those for BGaN and BAlN are reported first.
Alloying of BN with GaN and AlN, respectively, was achieved at a temperature of 1000°C and a pressure of 100 torr. Trimethylgallium (TMG), Trimethylaluminum (TMA), Triethylboron (TEB) and Ammonia (NH_3) were used as III and V precursors respectively. The BGaN and BAlN alloys layers were grown on 0.9 µm thick AlN-on-sapphire templates for the optical analysis described below. The BAlN/AlN mirrors were also grown on AlN-on-sapphire templates. The typical thickness of layers was around 160 nm. Boron incorporation was controlled through the molar ratio of TEB to the total molar concentration of the group III sources (TMG+TEB for BGaN, TMA+TEB for BAlN), denoted below as TEB/III. A detailed description of the optimized growth procedures for BGaN is given in reference[7]. The BGaN/GaN Distributed Bragg mirrors were grown on 3.5µm-thick GaN templates using the same growth conditions as the simple layers grown on AlN. The BInGaN quaternary alloys, on the other hand, were grown at a relatively low temperature.
ZnO thin films were grown on Si (111) substrates by Pulsed Laser Deposition (PLD), as described previously[8]. Growth of InGaN on such ZnO templates by MOVPE was demonstrated in prior work [4,8]. In this work, the MOVPE growth on the ZnO buffers was achieved by adapting the procedure in order to achieve alloying of BN with InGaN. This was accomplished at a relatively low temperature of 730°C. using Trimethylgallium (TMG), Trimethylindium (TMIn) as element III precursors with the addition of Triethylboron (TEB). A specific mixture of ammonia (NH_3) and Dimethylhydrazine (DMHy) was employed as a precursor for atomic N. DMHy was used to enhance the V/III ratio in the reactor at 730°C. DMHy has a much lower decomposition temperature than ammonia. Nitrogen was employed as a carrier gas during the whole growth process, in order to avoid back-etching of the ZnO and enhance indium incorporation [9]. Further details as well as compositional characterization procedures are given in reference [10].

3. RESULTS

A. BGaN refractive index and BGaN/GaN DBR reflectivity

High-Resolution X-Ray Diffraction was used to determine the boron content in the solid phase of the BGaN layers. Reciprocal Space Maps of the asymmetric (114) reflection showed that the layers were completely relaxed. The composition was estimated from the spacing of the diffraction peaks in 2θ-ω scans of symmetric (002) reflections using Vegard's Law. The boron content of the BGaN layers was found to vary between 0 and 1.3%.
Two-step ellipsometry and reflectance measurements allowed derivation of the refractive indexes of the BGaN layers. The following methodology was used: first, ellipsometry data was fitted to the Tauc-Lorentz model and then the alloys' refractive index was deduced from the model. Next, the extracted model was validated and fine-tuned by fitting to the interference fringes of experimental reflectance spectra. Only minor adjustments to the model were necessary for the ellipsometric and reflectance data to agree.
Figure 1 shows the resulting refractive index of BGaN films as a function of wavelength for various boron contents.

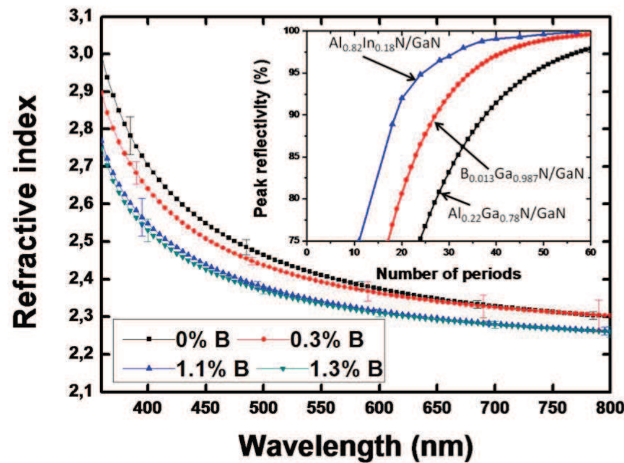

Figure 1 : Refractive index of BGaN epitaxial films grown on AlN templates as a function of wavelength. The inset represents the theoretical maximum reflectivity of BGaN/GaN DBR compared to AlGaN/GaN and AlInN/GaN structures as a function of the number of periods in the structure.

The spectra present two interesting features: first, the refractive index dramatically increases with increasing B concentration, in stark contrast to the evolution of the band gap. Just 1% boron content is thus enough to create a refractive index contrast of more than 0.1 between GaN and BGaN. To underline the impact of the boron addition, this effect was compared to that in the well-characterized material, AlGaN, which would require 22% of Al to achieve the same refractive index contrast with GaN [11].
Such high index contrast makes BGaN a material of great interest for the development of highly reflective DBRs. The reflectivity of each layer is directly proportional to the index contrast. Thus, fewer periods are required in order to achieve a highly reflective DBR with BGaN/GaN when compared to an AlGaN/GaN DBR. This is shown in the inset in figure 1, where the theoretical maximum reflectivity of a $B_{0.013}Ga_{0.987}N$/GaN DBR, (calculated using the model deduced above) is compared to the reflectivity of $Al_{0.22}Ga_{0.78}N$/GaN and lattice-matched $Al_{0.82}In_{0.18}N$/GaN [12] structures. BGaN/GaN is thus shown to be a viable alternative to AlGaN/GaN structures.
Moreover, there is a lattice mismatch of only 0.2% between $B_{0.01}Ga_{0.99}N$ and GaN, so the relaxation and cracking which are typically observed in AlGaN based mirrors due to build up of tensile strain should not be an issue. A nearly lattice-matched structure can thus enable the growth of high quality active regions for VCSEL structures.

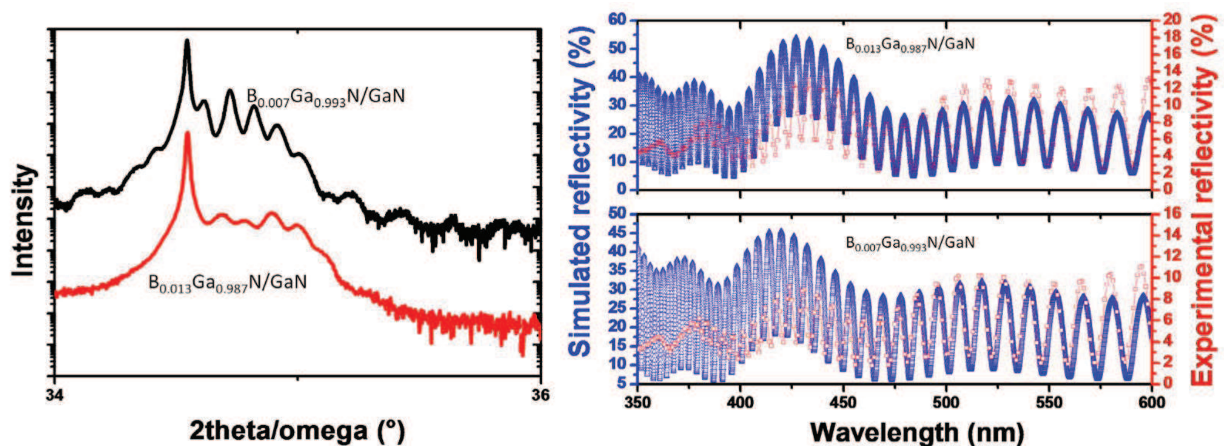

Figure 2 : (Left hand side) X-ray diffraction 2theta/omega spectra for two BGaN/GaN 6 period DBRs on a GaN template. (Right hand side) Experimental and simulated white light reflectivity spectra for two BGaN/GaN DBR structures.

These theoretical results provided the motivation behind the growth of BGaN-based DBRs. A structure consisting of a 6 period BGaN/GaN stack was grown on a GaN template. Each period was 40nm thick and the structure was designed for a passband centered around 420nm. X-ray diffraction 2θ-ω scans of the 6 period $B_{0.007}Ga_{0.993}N$/GaN and $B_{0.013}Ga_{0.987}N$/GaN DBRs (shown in figure 2 (left)) show the presence of satellite peaks, an indicator of good, albeit imperfect, crystalline quality. The angular spacing between the peaks confirmed the periodicity of the structure. The right hand side of Figure 2 presents the experimental and simulated reflectivity for BGaN/GaN DBRs containing 0.7 and 1.3% of boron. Simulated data was obtained using the transfer matrix method and the BGaN dispersion model discussed previously. The impact of the B content on the reflectivity peaks at 420 nm was clearly observed. In comparison to the peak reflectivity of $B_{0.007}Ga_{0.993}N$/GaN (around 7%) the peak reflectivity nearly doubled for the second structure (reaching 13%). The experimental curves are compared to simulated curves. An excellent agreement between the two was observed for a peak reflectivity at 420nm. However, there is still a discrepancy between experimental and simulated curves of peak reflectivity: the experimental value is 4 times lower than that predicted by the simulation. This was attributed to imperfect interfaces between BGaN and GaN. Nevertheless, the large increase in the reflectivity observed for a small increase in boron content is very promising for DBR development.

B. BAlN/AlN optical properties

As mentioned previously, BAlN is a novel material and very few studies have explored its optical properties and, more specifically, its refractive index. Indeed, an accurate knowledge of such data is essential for microcavity design, notably in predicting the layer thickness and simulating the DBR reflectivity. In order to obtain such accurate measurements, the BAlN samples were analyzed using ellipsometry in a UVISEL phase-modulated ellipsometer. The evaluation of I_c and I_s, linked to the Fresnel amplitudes of the reflection coefficients of the sample, yielded the required precision. The measurements were performed between 250nm and 800nm at a 70° incidence. Though information-rich, ellipsometry is an indirect measurement technique and requires fitting of the experimental data to a model calculated from the sample. In this case, the Jellison-Modine approach (based on the Tauc-Lorentz (TL) model) was adopted because it is an accurate model when interpreting SE spectra [13]. Among several other advantages, this approach also gives an estimate of the material's bandgap.
Chi-squared (χ^2) fitting was used to find the optimal fitting parameters to the model. The Levenberg Marquadt algorithm was used to implement it since it is the best suited for the fitting of ellipsometric spectra. The layer was modeled as a five-phase (Al_2O_3/AlN/BAlN/Surface roughness/air) system. Atomic Force Microscopy (AFM) was used in tapping

mode, in order to estimate the RMS roughness of the samples. Effective medium theories, such as the Bruggeman approximation then allowed the incorporation of the roughness in the ellipsometry model.
Figure 3 shows the experimental and calculated Ic and Is at different wavelengths for a sample. Good agreement between calculated (solid lines) and experimental (dotted lines) spectra was observed. The obtained χ^2 valu indicates that the assumed model and consequent results are reliable.

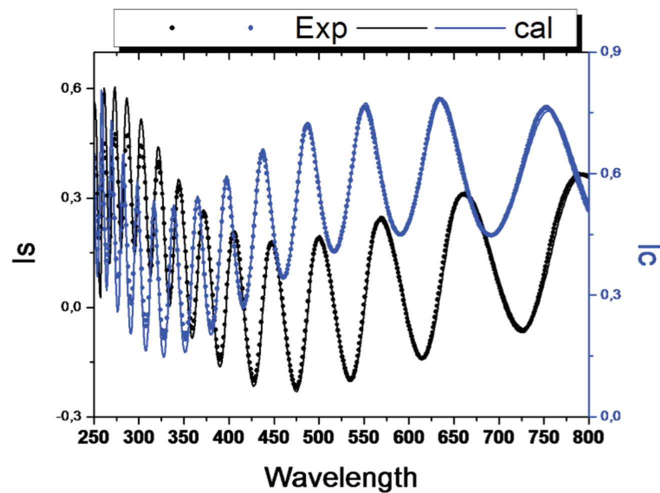

Figure 3 : Comparison between measured (dotted lines) and calculated (solid lines) ellipsometric spectra (Is and Ic) of a sample (TEB/III = 70%).

Figure 4 presents the refractive index as a function of wavelength for BAlN films with different ratios of the boron precursor in the gas phase (TEB/III).

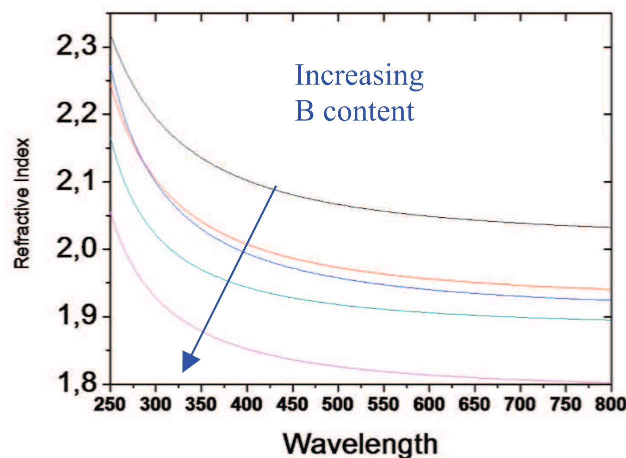

Figure 4 : Refractive index vs wavelength for $B_xAl_{1-x}N$ obtained from the different samples

A higher contrast was observed between AlN and BAlN than when comparing to conventional AlGaN layers.
Combining both the high refractive index contrast of BAlN (with respect to AlN and BalN) and the deep UV transparency, a 24-pair BAlN/AlN DBR (35 nm/31 nm) centered at 282 nm, was grown on an AlN template. The experimental reflectivity spectrum exhibited a peak reflectivity of 60% at 282 nm and a bandwidth of 15 nm.

C. BInGaN on ZnO-buffered Silicon

Figure 5 presents the 2θ-ω HR-XRD spectrum for a BInGaN/ZnO/Si (111) sample (in blue). As a means of comparison, the spectrum has been superimposed to that of an InGaN/ZnO/Si (111) sample grown under similar conditions but without TEB (red). In both cases, the most intense peaks correspond to the wurtzite (0002) reflection of the ZnO buffer layer. The two less intense peaks correspond to BInGaN (blue) and InGaN (red) (0002) reflections, respectively. Vegard's law and SIMS measurements[8] suggest that the InGaN layer contains approximately 19.5% In, which makes its c-axis lattice parameter larger than that of ZnO. This indicates that there would be tensile strain and misfits in the InGaN layer. Note that the introduction of boron results in the decrease of the c lattice parameter and a reduction of the tensile strain, as expected. This suggests that boron addition can be used to maintain lattice-matching conditions at In percentages higher than 18%.

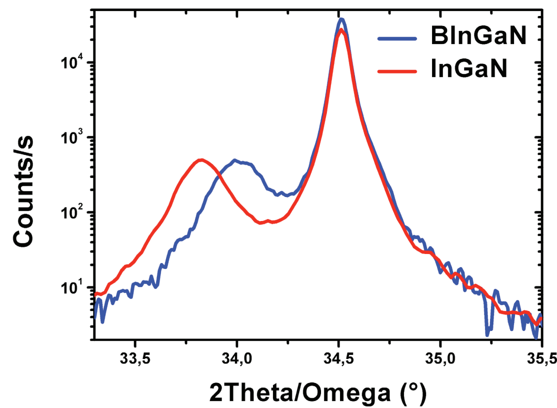

Figure 5 : X ray diffraction 2 theta/omega scan for BInGaN layers grown on ZnO/silicon templates for TEB/III = 0% and 2.6%

The incorporation of boron in the layers was confirmed by SIMS profiling along the growth direction. The resulting profile is shown in figure 6. It exhibits a uniform boron distribution in the BInGaN layer. Along the growth direction, the Ga concentration varies simultaneously with those of In and B, which indicates that In, B and Ga atoms are mixed in the lattice. The tails observed after the step were attributed to instrumental artifacts. They may correspond to the formation of metal droplets which "float" at the bottom of the SIMS crater during the profiling.

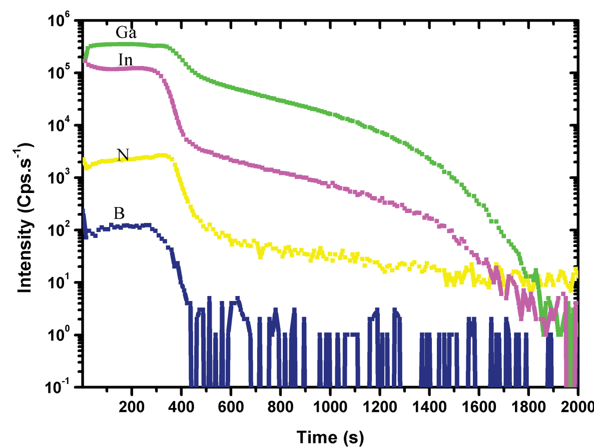

Figure 6 : SIMS profile obtained for a 140 nm thick BInGaN layer grown on a ZnO-buffered Si substrate.

The composition measurement of quaternary BInGaN is not straightforward because of the relatively low boron content in these samples. Therefore, a reference database was created using ternary alloys of InGaN and BGaN with various indium and boron contents. The indium and boron concentrations were estimated to a high accuracy using HR-XRD and they were used to calibrate SIMS for quantitative measurements of boron and indium in the BInGaN layers. The results were then crosschecked by X-ray photoelectron spectroscopy XPS. This approach was developed in detail for the analysis of BInGaN grown on GaN (discussed in reference [11]) and applied to BInGaN/ZnO samples. Based on this calibration, it was found that an increase of the TEB flow in the growth chamber from 0 to 6.54 sccm led to B and In content variations in the solid phase from 0 to 2% and 19.5 to 14%, respectively.

4. CONCLUSION

In this work, optical properties of dilute BGaN and BAlN layers grown on AlN template substrates by MOVPE were investigated. The refractive indices were determined using a two-stage technique based on ellipsometry. A relatively large refractive index variation was observed between both BGaN/GaN and BAlN/AlN with values exceeding 0.1 and 0.25, respectively. As a result, it was shown that fewer periods are needed in boron-based nitrides in order to reach a high DBR reflectivity compared with typical AlGaN/GaN DBRs.

The potential of boron-based nitrides for visible range solar cells applications was also demonstrated through the example of BInGaN growth on ZnO-buffered silicon substrates. It was found that through boron introduction reduced lattice mismatch, and thus reduced tensile strain, could be obtained for high In contents.

References

[1] S. Sakai, Y. Ueta, Y. Terauchi, Jpn. J. Appl. Phys. 32 (1993) 4413.

[2] D. S. McGregor, T.C. Unruh, W. J. McNeil, Nuclear Instruments and Methods in Physics Research A 591 (2008) 530–533.

[3] O. Jani, I. Ferguson, C. Honsberg, and S. Kurtz, Appl. Phys. Lett. 91 (2007) 132117.

[4] D. J. Rogers et al., Appl. Phys. Lett. 91 (2007) 071120

[5] C.H. Wei and J.H. Edgar, J. of Crystal Growth 208 179-182 (2000)

[6] L. K. Teles , J. Furthm , A. Tabata , J. R. Leite , F. Bechstedt , T. Frey , D.J. As , K. Lischka, Physica E 13 (2002) 1086 – 1089

[7] A. Ougazzaden, et al., J. Crystal Growth (2006), doi:10.1016/j.jcrysgro.2006.10.072

[8] A. Ougazzaden et al., Proc. of SPIE Vol. 7603 (2010) 76031D-1

[9] F. Scholz et al., J. Crystal Growth 170 (1997) 321

[10] S. Gautier et al., J. Crystal Growth 312 (2010) 641-644

[11] D. Brunner, et al, J. Appl. Phys., 82 (1997) 5090.

[12] J. F. Carlin et al, Appl. Phys. Lett., 86 (2005) 031107

[13] G. E. Jr Jellison et al, Appl. Phys. Lett., 69 3 (1996) 371